Origins of linewidth in ^{1}H magic-angle spinning NMR

Vadim E. Zorin
Department of Chemistry, Durham University, South Road, Durham, DH1 3LE, United Kingdom

Steven P. Brown
Department of Physics, University of Warwick, Coventry, CV4 7AL, United Kingdom

Paul Hodgkinson[a)]
Department of Chemistry, Durham University, South Road, Durham, DH1 3LE, United Kingdom

(Received 27 June 2006; accepted 29 August 2006; published online 10 October 2006)

A detailed study of the factors determining the linewidth (and hence resolution) in ^{1}H solid-state magic-angle spinning NMR is described. Although it has been known from the early days of magic-angle spinning (MAS) that resolution of spectra from abundant nuclear spins, such as ^{1}H, increases approximately linearly with increasing sample rotation rate, the difficulty of describing the dynamics of extended networks of coupled spins has made it difficult to predict *a priori* the resolution expected for a given sample. Using recently developed, highly efficient methods of numerical simulation, together with experimental measurements on a variety of test systems, we propose a comprehensive picture of ^{1}H resolution under MAS. The "homogeneous" component of the linewidth is shown to depend primarily on the ratio between an effective local coupling strength and the spin rate, modified by geometrical factors which loosely correspond to the "dimensionality" of the coupling network. The remaining "inhomogeneous" component of the natural linewidth is confirmed to have the same properties as in dilute-spin NMR. Variations in the NMR frequency due to chemical shift effects are shown to have minimal impact on ^{1}H resolution. The implications of these results for solid-state NMR experiments involving ^{1}H and other abundant-spin nuclei are discussed. © *2006 American Institute of Physics*. [DOI: 10.1063/1.2357602]

I. INTRODUCTION

The principal hurdle in applying solid-state NMR to typical organic compounds is the presence of strong dipolar couplings between the protons. These are averaged to zero by rapid isotropic reorientation in solution-state NMR, resulting in narrow well-defined ^{1}H resonances that are only influenced by the isotropic chemical shift and J couplings. In solid samples, however, the dipolar couplings are not significantly motionally averaged and the presence of an extensive network of dipolar couplings results in broad and featureless proton line shapes (typically about 100 kHz wide). But since the NMR interactions transform as rank 2 tensors, spinning samples at an angle $\theta_m = 54.7°$ with respect to the static magnetic field [the angle that zeroes the second order Legendre polynomial, $(3\cos^2\theta - 1)/2$] has the effect of averaging the anisotropic interactions. In general this averaging is only partial since it is not possible (with existing spinner technology) to spin samples very much faster than the width of the unaveraged spectrum. The appearance of the spectrum then depends strongly on the nature of the Hamiltonian for the NMR interaction responsible for the width of the spectrum. In the case of so-called "inhomogeneous" interactions, such as the chemical shift anisotropy and *heteronuclear* dipolar interaction, the evolution of the density matrix is perfectly refocused over a rotation cycle, leading to sharp spectral features—center bands at the isotropic NMR frequency plus spinning sidebands separated by multiples of the rotation frequency.

The Hamiltonian for the dipolar couplings between a system of more than two like spins behaves very differently. The Hamiltonian for a set of dipolar coupled nuclear spins is

$$H_{\text{dipolar}}(t) = \sum_{j<k} d_{jk}^{\Omega}(t) T_{jk}, \tag{1}$$

$$T_{jk} = 2I_{jz}I_{kz} + \frac{1}{2}(I_{j+}I_{k-} + I_{j-}I_{k+}), \tag{2}$$

where the instantaneous dipolar coupling between a pair of spins, d_{jk}^{Ω}, is time dependent due to the sample spinning. Except in the special case (considered in Sec. III C) in which the dipolar tensors share a common axis system, the different terms of H_{dipolar} do not commute since the spin terms T_{jk} do not, in general, commute with each other ($[T_{jk}, T_{kl}] \neq 0$ for $j \neq l$). As a result, the Hamiltonian for homonuclear dipolar coupling network is "homogeneous" under sample spinning,[1] since it does not commute with itself at different points in the rotation cycle, $[H(t), H(t')] \neq 0$. As a consequence, the spectral features (centerbands and spinning sidebands) have a finite width which only decreases relatively slowly with increasing spin rate.

In spite of these limitations, specific ^{1}H resonances can be resolved for small to moderately sized organic molecules under fast magic-angle spining (MAS) (greater than about 25 kHz) and at high magnetic field (greater than about 400 MHz).[2] This resolution is sufficient, for example, to

[a)]Electronic mail: paul.hodgkinson@durham.ac.uk

identify correlation peaks due to proton-proton proximities in two-dimensional ^{1}H double-quantum (DQ) MAS spectra, with applications including probing hydrogen bonding in self-assembled polymeric structures,[3] pharmaceutical systems,[4] small biomolecules[5] and inorganic complexes,[6] as well as the role of aromatic π-π interactions in determining packing[7,8] and host-guest interactions for a molecular tweezer.[9] Understanding the factors that determine ^{1}H resolution in solid-state NMR is key to further applications of ^{1}H NMR to new structural problems.

Unfortunately, the homogeneous nature of the homonuclear coupling Hamiltonian is a major challenge for theoretical descriptions of dipolar coupling networks. Exact treatments seek to determine features of the ^{1}H spectrum, such as linewidths, starting from the complete system Hamiltonian (although generally neglecting chemical shift differences). For instance, average Hamiltonian theory has been used to develop a theory of proton linewidths under MAS.[10] Determining the average Hamiltonian over the MAS rotor period obscures, however, the different behaviors of center bands and spinning sidebands (these differences are discussed further in Sec. III D below). This limitation can be overcome, at the expense of significantly increased complexity, using Floquet treatments.[11–13] In general, however, exact treatments rapidly become intractable once more than two spins are involved. The resulting expressions provide little insight into the factors that determine what the effective ^{1}H resolution will be for a given sample and set of experimental conditions.

A common alternative approach to an exact analysis involves treating the effects of spin flips due to the couplings in stochastic terms using empirical memory functions,[14] and this approach has been extended to proton spin dynamics under MAS.[15] In a similar vein, the effect of proton-proton couplings on ^{1}H heteronuclear decoupling has been usefully modeled in Liouville space using a superoperator representing spin diffusion.[16] Although such approaches often provide good *models* for the observed behavior, they generally invoke empirical parameters, such as a rate constant for "spin diffusion," and so lack predictive power; a true *ab initio* description would be able to predict the ^{1}H linewidth simply starting from a specification of the coupling network and the experimental conditions.

Numerical simulations would seem to avoid the complexities of exact analytical treatments of coupled spin systems. However, conventional simulation techniques are poorly adapted for this task, as the computational burden increases rapidly with the number of protons in the nuclear spin system (approximately as 2^{3n}, where n is the number of spins). Efficient simulation codes which take advantage of the relatively high sparsity of the nuclear spin Hamiltonian under free precession, such as SPINEVOLUTION,[17] can work with up to about ten nuclear spins subject to MAS. This is about the minimum needed to obtain realistic proton line shapes (see below), but the calculation times are still becoming prohibitive. Other published attempts to calculate *ab initio* proton spectra under MAS have involved Floquet methods.[13] Unfortunately, these scale particularly badly with increasing spin system size, and so the limit in this case was about seven nuclear spins.

As we have previously described, however, the efficiency of numerical simulation can be greatly increased if the intrinsic periodic symmetry of a crystalline lattice is exploited.[18,19] By symmetrizing the Hamiltonian with respect to the translational symmetry, the Hamiltonian can be further block diagonalized, improving the calculation speed by orders of magnitude. This either allows the number of spins considered to be significantly increased or permits a much larger number of simulations to be carried out in a fixed period. In this paper, we describe how such calculations have been used, together with experimental measurements on a variety of model systems, to determine the relationship between the dipolar coupling network, the sample spinning rate, and the resulting ^{1}H linewidths under magic-angle spinning.

After introducing the experimental and numerical tools in the following section, Sec. III shows how the homogeneous linewidth due to the ^{1}H dipolar coupling network can be rationalized. ^{1}H linewidths will also contain inhomogeneous contributions due to factors such as (static) disorder, bulk susceptibility broadenings, etc. These factors are considered in Sec. IV. The final section considers other possible contributions to proton linewidths, particularly whether chemical shift differences or anisotropies can have a significant impact, and discusses how these results for ^{1}H can be applied to other abundant nuclear spins such as ^{19}F and ^{31}P.

II. METHODS

A diverse range of powdered microcrystalline samples was chosen for experimental study, as set out in Table I. Alanine, glycine, and malonic acids are typical organic molecular solids with a range of ^{1}H environments and relatively strong dipolar coupling networks. In contrast, the overall dipolar coupling strength is significantly weaker in adamantane and hexamethylbenzene (HMB) due to internal motions, while the coupling network in d_{16}-adamantane (96% deuterium enrichment) is extremely weak due to the low concentration of protons (in addition to the averaging of intramolecular couplings due to internal motion). HMB is also an example of a system with large inhomogeneous broadenings; the presence of stacked aromatic rings leads to a large anisotropy of the magnetic susceptibility (Sec. IV).

The "effective dipolar coupling" experienced by a given proton site, j, can be expressed quantitatively using the root-sum-square coupling,

$$d_{\mathrm{rss},j} = \sqrt{\sum_{k \neq j} d_{jk}^2}, \tag{3}$$

where d_{jk} is the dipolar coupling strength between spins j and k. This can be regarded as a site-specific generalization of the second moment which is widely used to express the dipolar coupling strength in static samples where individual H sites are not resolved.[20] We and others have previously discussed the significance of this parameter and its quantification from the ^{1}H NMR spectrum.[12,19] Table I gives estimates of d_{rss} for the different resolved ^{1}H sites. In most cases

TABLE I. Compounds used in experiments and estimated values of root-sum-squared dipolar coupling for different ^{1}H sites.

Compound	Chemical structure	d_{rss} / kHz	Comments
adamantane (ADAMAN03)		6.1[b]	Intramolecular dipolar couplings removed by rapid molecular tumbling, leaving only the relatively weak intermolecular couplings
96%-*d*-adamantane		CH_2: 1.2[a] CH: 1.2[a]	Mean coupling strength reduced further by high level of deuteration
alanine	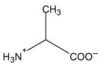	CH: 18[a] CH_3: 19[a] NH_3^+: 20[a]	Prototypical organic solid
hexamethylbenzene	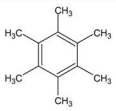	9.1[a]	Mean coupling strength reduced by fast methyl group reorientation and the molecular rotation around the six-fold axis
malonic acid (MALNAC06)	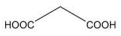	COOH: 14[c] CH_2: 23[c]	The different proton sites have significantly different mean coupling strengths
d-urea·decanoic acid		CH_2: 10[a]	Rapid rotation of the decanoic acid molecules around the axis of the tunnel structure created by the urea creates a quasi-one-dimensional spin system

[a]Estimated by fitting spinning sideband intensities of the ^{1}H MAS spectrum.
[b]Estimated from atomic positions derived from XRD data from the Cambridge Structural Database (reference code in parentheses).
[c]Estimated from atomic positions derived from neutron scattering data from the Cambridge Structural Database (reference code in parentheses).

these have been estimated from atomic positions derived from x-ray diffraction (XRD) or, where possible, neutron scattering data (since the latter technique localies H atoms with much greater accuracy). It is important to note, however, that the resulting d_{rss} values are extremely sensitive to errors in measuring short H–H distances; interproton distances of less than 1.75 Å have been adjusted to a fixed value of 1.75 Å to facilitate consistency of comparison. As discussed further in Sec. III B, these uncertainties in estimating d_{rss} complicate the comparison of calculated and experimental linewidths. Moreover, vibrational averaging is known to lead to systematic differences between distances obtained from diffraction and those derived from dipolar couplings.[21] Except in the case of adamantane, where these factors are not relevant, the values of d_{rss} given above should therefore be interpreted cautiously, since the uncertainties are estimated at about 10%. In cases where extensive motional averaging complicated the calculation of d_{rss} from atomic positions, its value was estimated from fitting the spinning sideband intensities of the ^{1}H MAS spectrum to a spin pair model.[19] A similar level of uncertainty is predicted for these NMR measurements.

The "geometry" of the proton network is also expected to play an important role in the relationship between the dipolar coupling network and the observed linewidths. The inclusion systems formed between linear molecules and urea are interesting examples of quasi-one-dimensional arrangements,[22] where rapid rotation of the guest molecules about their axis means that the dipolar couplings within guest molecules are averaged to their projections along the rotation axis. We have used the inclusion compound formed between deuterated urea and decanoic acid, where deuteration of the urea reduces intermolecular couplings and reinforces the linear nature of the spin system.

The NMR experiments used in this study are particularly straightforward (Fig. 1). The "natural linewidth" was measured from the full width at half maximum (FWHM) of simple pulse-and-acquire ^{1}H spectra [Fig. 1(a)]. The homogeneous contribution to this linewidth was measured using a simple $\tau-\pi-\tau$ spin-echo experiment (with the τ values synchronized to multiples of the rotor period to avoid modulations as a function of the rotor phase). The intensity of the centerband peak was measured as a function of 2τ and fitted to a decaying exponential to obtain a phenomenological T_2 value [Fig. 1(c)]. The "spin-echo linewidth" is then $1/\pi T_2$. The term spin-echoline width is used hereafter for this quantity since the physical significance of terms such as "homogeneous linewidth" is not clear, especially when strong sidebands are present (this is discussed further in Sec. III D). This terminology also avoids confusion with the distinction between Hamiltonians that are homogeneous versus inhomogeneous under sample spinning (as discussed in the Introduction). The natural and spin-echo linewidths were measured as a function of MAS spin rate and static magnetic field for

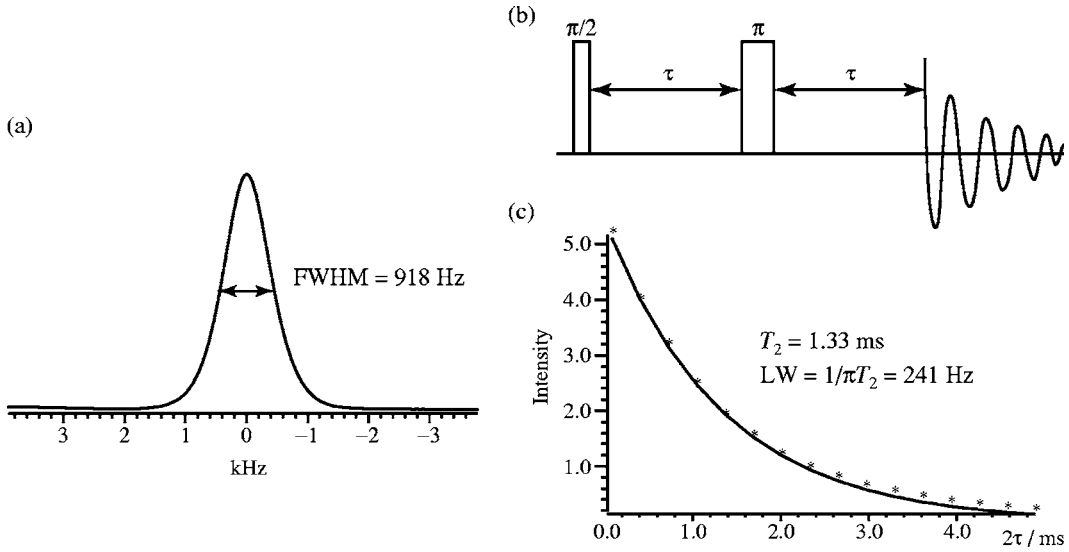

FIG. 1. (a) The "natural linewidth" of the resonances was measured from their full width at half maximum (FWHM). (b) The "homogeneous" (or "spin-echo") linewidth was measured from the intensity of a spin echo as a function of the spin-echo delay τ and (c) fitting the resulting decay to a simple exponential. Data shown are for hexamethylbenzene at a MAS rate of 25 kHz and a ^{1}H Larmor frequency of 800 MHz.

each of the selected systems. The different fields and MAS probes used are listed in Table II. As shown in the following section, this allows us to build up a comprehensive picture of the factors that determine ^{1}H resolution under magic-angle spinning.

The principles behind the numerical simulations have been described elsewhere[18,19] and will be only briefly summarized here. We consider periodic systems based on a "unit cell" with a small number of spins. This is translated along one or more axes to generate a periodic lattice, and the couplings between the spins are calculated using this geometry. Periodic boundary conditions are imposed to ensure that the couplings experienced by the different unit cells are identical. The resulting nuclear spin Hamiltonian must share this symmetry, and so must be block diagonal *when expressed in a suitable symmetry-adapted basis*. With N unit cells, the original Hamiltonian will be divided into N blocks with the symmetry-adapted states being distributed fairly evenly between the blocks. Since the time-consuming steps (diagonalization, matrix multiplication, etc.) of numerical simulations are $O(n^3)$ processes, the division into N blocks approximately a factor of N smaller results in time saving of a factor of about N^2. The reduction in matrix size also permits larger problems to be considered. In particular, it is now feasible to verify that the behavior converges to a well-defined limit as the number of cells increases.

III. SPIN-ECHO LINEWIDTHS UNDER MAGIC-ANGLE SPINNING

Figure 2 collates the results of experimental measurements of the spin-echo linewidth of the center band as a function of magic-angle spinning rate for the different systems studied. Semianalytical theories[10] predict that the ^{1}H linewidth should scale inversely with spin rate ν_r, and so the plot shows linewidth versus $1/\nu_r$. Both horizontal and vertical axes have been made dimensionless by "normalizing" against the effective dipolar coupling strength as measured by the root-sum-square coupling. This allows linewidths from systems with very different mean coupling strengths to be directly compared.

At first sight, there seems little pattern to the overall distribution of data points. Further examination, however, reveals clear trends. For a given sample, the ^{1}H linewidth is *approximately* inversely proportional to the magic-angle spin rate, with the relationship between the center band spin-echo linewidth and MAS rate given by

$$\mathrm{FWHM} \approx G\frac{d_{\mathrm{rss}}^2}{\nu_r}, \tag{4}$$

where G is a constant of proportionality that varies between samples. Note how the linewidth under magic-angle spinning scales as the *square* of the effective coupling strength d_{rss}. This contrasts with the dipolar linewidth for static samples and the pattern of sideband intensities in spinning samples

TABLE II. Summary of equipment used. (Figures in parentheses are the maximum sample spinning rates used for each probe.)

^{1}H Larmor frequency and make	MAS probes (rotor outside diameter) used
300 MHz (Varian UnityPlus)	2.5 mm (30 kHz)
500 MHz (Varian InfinityPlus)	2.5 mm (29 kHz), 3.2 mm (22 kHz), 5 mm (4 kHz)
600 MHz (Varian Infinity)	1.8 mm (40 kHz)
800 MHz (Varian InfinityPlus)	2.5 mm (25 kHz)

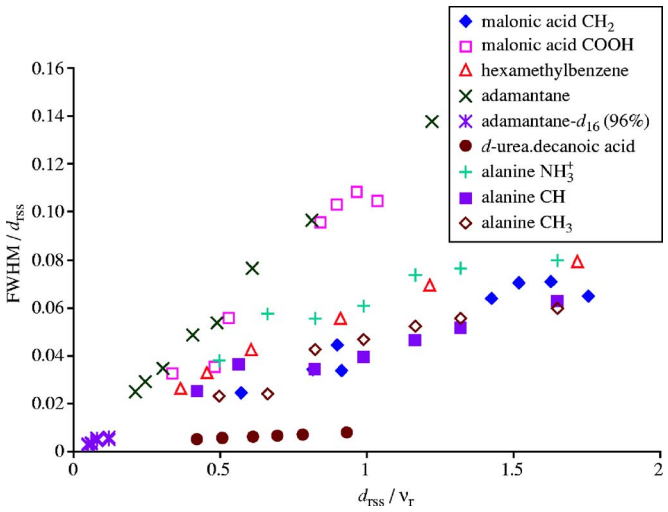

FIG. 2. (Color online) Plot of spin-echo linewidths vs inverse spin rate for the systems studied, normalized by the d_{rss} values shown in Table I. The measurements are compiled from experiments taken at different static magnetic fields and with different NMR probes (see Ref. 50 for full details).

which scale linearly with the coupling strength.

It is useful to consider the effect of isotopic dilution of ^{1}H by ^{2}H in terms of the above relationship, given the potential importance of this approach to the solid-state NMR of microcrystalline biomolecules.[23–25] If we can treat the collection of H atoms around a given ^{1}H as a continuous distribution, with $\rho(\tau)d\tau$ being the probability of finding a ^{1}H spin in the volume element, $d\tau$, then the root-sum-square coupling of the diluted network is given by

$$d_{rss}(\rho) = \sqrt{\int_{\tau} \rho(\tau) d(\tau)^2 d\tau}, \tag{5}$$

where $d(\tau)$ is the coupling strength between the reference ^{1}H at the coordinate origin and a ^{1}H at position τ. We can neglect the dipolar coupling to the ^{2}H nuclei since this coupling is heteronuclear and will be refocused by the spin echo. If we assume that the substitution is random, i.e., ρ is independent of τ, then the effective coupling strength in the diluted sample is readily expressed in terms of d_{rss} for the nondiluted sample

$$d_{rss}(\rho) = \sqrt{\rho} d_{rss}. \tag{6}$$

For example, the d_{rss} values for adamantane and 96%-*d*-adamantane in Table I are 6.0 kHz (calculated from x-ray structure) and 1.2 kHz (estimated from NMR), respectively. The ratio of d_{rss} values agrees exactly with $\sqrt{0.04}=0.2$, where $\rho=4\%$. Hence the spin-echo linewidth, from Eq. (4), is expected to scale approximately linearly with ρ. The relationship cannot be perfectly linear since the overall "structure" of the ^{1}H network, as measured by G, will also be a function of the level of deuteration. Note how the slope of the data points for the deuterated adamantane sample in Fig. 2 is distinctly different from that of the fully protonated adamantane since the network in the diluted system no longer has a cubic symmetry and more closely resembles the "intermediate geometry." This treatment in terms of a "continuous proton density," which allows ρ to be extracted as a constant parameter, may break down if the coupling network has a strong "local structure." d_{rss} in an isolated CH_2 group, for example, will strongly depend on whether the other H atom is ^{1}H or ^{2}H, and it would be more appropriate to describe the NMR spectrum for the diluted system in this case as the sum of the responses from C^1H^2H and C^1H_2. These conclusions agree with recent experimental work in which the ^{1}H linewidth was found to increase monotonically with the degree of protonation.[29]

These relationships between spin-echo linewidth and magic-angle spinning rate are consistent between samples with very different mean coupling strengths. For instance, the curves formed from the data points from adamantane and the acid proton of malonic acid are very close, as are the data points from hexamethylbenzene and the NH_3^+ of alanine. This confirms the utility of the normalization against d_{rss}, and allows us to use data from mobile systems to extrapolate the dependence on MAS for rigid compounds to faster spin rates than currently (or physically) available.

An important deduction from this ability to linearly extrapolate towards infinite spin rate is that the spin-echo linewidth for all the sample studies appears to decrease to zero in this limit. This is even true for the deuterated adamantane sample where spin-echo linewidths as low as 5 Hz are observed at the highest MAS rates (see Ref. 50 for details). The limit of the spin-echo linewidth is expected to be set by J_{HH} couplings (which are not refocused by the spin-echo) and spin-spin relaxation (T_2). J_{HH} are generally small, but it is more surprising that the limit on resolution set by T_2 relaxation is too small to detect (in the presence of the linewidth due to the dipolar coupling network). This implies that the potential of solid-state NMR in organic systems is not limited by T_2 relaxation (as often assumed), but only the efficiency with which the homonuclear dipolar couplings can be suppressed, e.g., by MAS or isotopic substitution.

Another clear feature of Fig. 2 is that the proportionality coefficient between the local coupling strength and the spin-echo linewidth varies strongly between samples. However, these variations can be rationalized in terms of the geometrical arrangement of the coupled spins. For example, the arrangement of the protons in the urea inclusion systems is quasi-one-dimensional; rapid rotation about the tunnel axis means that all the intramolecular couplings are reduced to their "projection" along the rotation axis, while deuterium substitution of the host urea molecules strongly reduces intermolecular couplings. It is well known that such a one-dimensional arrangement of spins behaves inhomogeneously under magic-angle spinning. The couplings share a common set of principal axes, and so the dipolar coupling Hamiltonian [Eq. (1)] commutes with itself at different points in the rotor cycle, leading to a refocusing of the dipolar evolution over each rotation period.[1] It is not surprising, therefore, that the ^{1}H linewidth is much narrower in comparison to more typical systems with similar values of d_{rss}. In contrast, the cubic symmetry of the adamantane structure means that its network geometry is clearly three dimensional. This is associated with significantly broader lines for a given d_{rss}/ν_r ratio. The arrangement of protons within the malonic acid system lies somewhere in between, with strong dipolar cou-

plings within a CH_2 pair, but also significant couplings between the CH_2 units. The resulting linewidths are approximately half that expected from a corresponding "three-dimensional" (3D) system with the same d_{rss}. The linewidth for a given sample is therefore expected to lie in the range

$$G_{CH}\frac{d_{rss}^2}{\nu_r} \lesssim \text{FWHM} \lesssim G_{cubic}\frac{d_{rss}^2}{\nu_r}, \tag{7}$$

where the dimensionless constants $G_{CH}=0.04$ and $G_{cubic}=0.11$ have been obtained by linear regression of the data points for the CH of alanine and adamantane, respectively. This relationship and the "structure constants" are independent of the identity of the abundant spin (which only influences the effective coupling strength via the magnetogyric ratio). It should be emphasized, however, that Eq. (7) and the G coefficients given are simply intended as a rule of thumb for estimating likely ^{1}H linewidths for powder samples, as the linear relationship between linewidth and inverse spin rate is only an approximation (cf. Figs. 4 and 5).

In the following sections, we consider the different "network geometries" and attempt to predict the ^{1}H linewidth and its dependence on the magic-angle spinning rate. This is a key test of the hypothesis that ^{1}H solid-state NMR linewidths can be rationalized in terms of the strength of the dipolar coupling network modified by an overall effective "dimensionality."

A. 3D lattice: Adamantane

The three-dimensional lattice of adamantane is a particular challenge for exact modeling since the simulation of a true three dimensional network rapidly becomes intractable. For instance, a fragment of $3\times3\times3$ cells with one spin per cell involves 27 spins, while the limit for manageable computations of coupled spin systems under MAS is about 15 spins when exploiting periodic symmetry.[18] We have chosen instead to model the close-packed lattice of adamantane using a one-dimensional lattice with three spins per unit cell. These are arranged in an equilateral triangle with the spacing between cells matching the internuclear distances within the cell [Fig. 3(a)]. This is a questionable model for the true physical geometry, but it does capture something of the three-dimensional nature of the lattice, with each spin being coupled to four nearest neighbors at the same distance (the two other members of the unit cell plus the corresponding spin in the two neighboring unit cells). The coupling strength is matched to that of adamantane via the root-sum-square coupling. The d_{rss} has been calculated from the crystallographic data,[26] and the resulting value, $d_{rss}=6.08$ kHz, is in good agreement with a previous calculation[11] which considered only closest neighbors (i.e., most remote couplings make negligible difference to d_{rss}). The unique internuclear separation was then adjusted so that d_{rss} of the one-dimensional lattice matched 6.08 kHz (corresponding to a next-nearest-neighbor distance R of 3.44 Å).

Figure 3 shows simulated spectra using three and four unit cells (9 and 12 nuclei, respectively). Some individual transitions can still be resolved when only nine spins are involved, but the spectrum is otherwise essentially identical

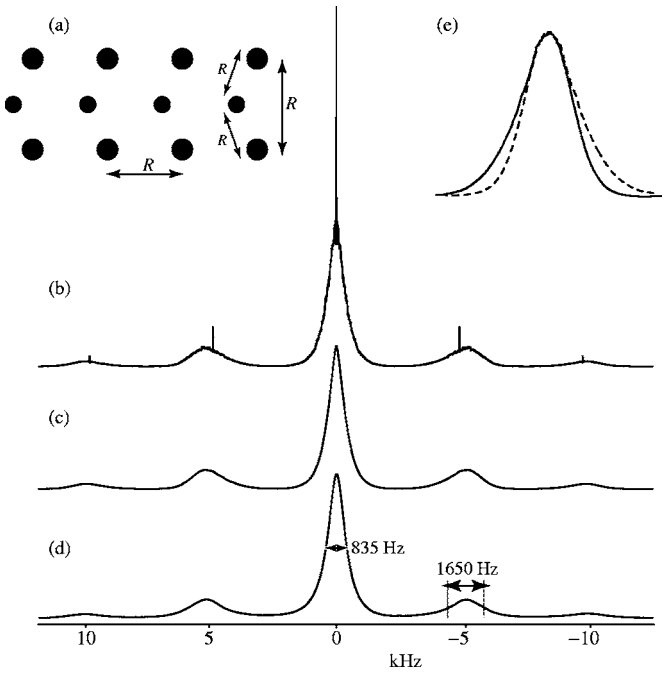

FIG. 3. Simulation of the ^{1}H adamantane spectrum with a magic-angle spinning rate of 5 kHz. (a) Schematic illustration of quasi-3D geometry used, and calculated spectra using (b) three unit cells and (c) four unit cells. (d) Corresponding experimental spectrum (measured at a ^{1}H Larmor frequency of 500 MHz). The centerband and sidebands have distinctly different widths, and the sidebands are distinctly asymmetric, as highlighted in (e) which overlays the −1 (dotted line) and +1 (solid line) sidebands. Other calculation parameters: spectral resolution (histogram bin width) of 312 Hz and 144 crystal orientations in the powder sum. As the Hamiltonian is purely dipolar, the spectrum is independent of the magnetic field and so the ^{1}H Larmor frequency is not significant.

to that calculated using four unit cells, i.e., the calculations have "converged" in the sense that further extensions of the spin system will have no visible effect on the spectrum at this resolution (set by the histogram bin width). Since the sharp features in Fig. 3(b) are easily ignored and the nine-spin calculation is much faster (6 min compared to 17 h on an Athlon 2800+PC), we used the three unit cell model in subsequent calculations.

As inhomogeneous contributions to the adamantane linewidth are negligible, we can directly compare these simulated spectra with the simple pulse-and-acquire spectrum obtained experimentally [Fig. 3(d)]. The agreement is remarkably good, particularly considering the distortions applied to the lattice to fit it within the one-dimensional framework of the calculations. It is also interesting to note that the spinning sidebands in both experimental and simulated spectra share a slight asymmetry [Fig. 3(e)], which might otherwise be attributed to poor "phasing" of the experimental spectrum (to obtain pure absorption line shapes). Although the overall spectrum from a purely dipolar Hamiltonian must be symmetrical and the sidebands must have the same phase (for an isotropic powder sample),[27] there is no theoretical requirement for the individual sidebands from a homogeneous Hamiltonian to be strictly symmetrical.

It is important to stress that the good agreement obtained between the experimental single-quantum spectrum and the simulation obtained with a 12-spin system does not imply

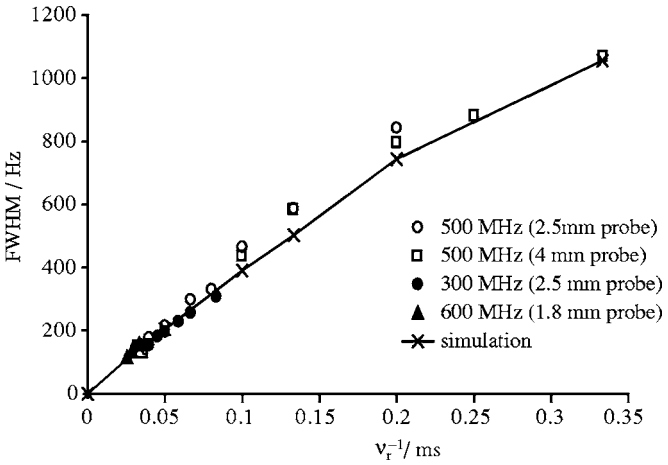

FIG. 4. MAS rate dependence of the adamantane linewidth taken under a variety of experimental conditions, and calculated centerband widths using the quasi-3D geometry (nine spins). Straight lines linking the calculated points are included as guides to the eyes.

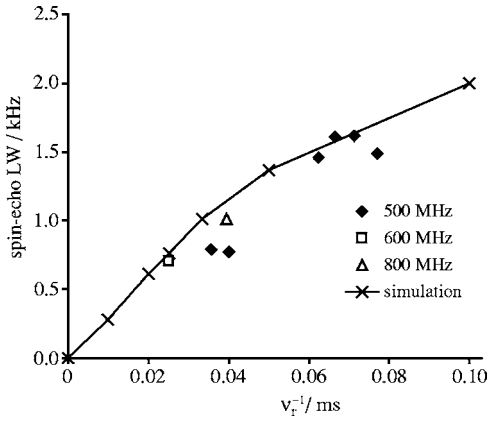

FIG. 5. Magic-angle spinning rate dependence of the experimental spin-echo linewidth of the malonic acid ^{1}H methylene signal and the calculated centerband width for a spin-pair model. The simulation used five cells of two spins per cell with an internuclear distance of 1.75 Å within the cell and 2.5 Å between cells. Straight lines linking the calculated points are included as guides to the eyes.

that such simulations are sufficient to describe all aspects of multi-spin dynamics. The evolution of the single-quantum coherence of a given spin is largely determined by the strong dipolar couplings to the spins in the immediate vicinity, and only a relatively modest number of spins are required to create a Hilbert space into which the single-quantum coherence can smoothly dephase. In contrast, multi-quantum coherences between several spins probe longer range and time scales and such "spin counting" experiments[28] will, by definition, require larger numbers of spins to be described correctly.

Figure 4 shows the MAS rate dependence of the calculated center band widths. Again these agree very well with experimental measurements, confirming that the simulations of the spin dynamics in the model network are sound. It is important to note that this comparison does not involve any adjustable parameters; the linewidth has been calculated purely on the basis of crystallographic information about the network geometry, independently of any NMR measurements. The agreement would be even more satisfying if the slope of the approximate line formed by the experimental and calculated points [corresponding to the G "structure factor" in Eq. (4)] could be predicted *ab initio*. Unfortunately, this is an extremely complex problem,[12] and the empirical relationship between the local coupling strength and the resulting linewidth given by Eq. (7) is sufficient to provide good estimates of the achievable resolution.

B. "Intermediate" geometries

It is clear from Fig. 2 that the behavior of systems such as the CH_2 protons in malonic acid is intermediate between the limiting cases of one- and three-dimensional geometries. We have chosen to model this system as a linear arrangement of spin pairs, with the internuclear distance between the pair matching the H–H distance within typical CH_2 units obtained from crystallographic data.[29] The intercell separation was then adjusted so that the overall root-sum-square coupling for an individual proton matched the d_{rss} for malonic acid given in Table I.

As shown in Fig. 5, the agreement between the calculated and experimental spin-echo linewidths is again good. The differences between the mean of the experimental and calculated data points are actually smaller than the variations between experimental points; for reasons that are not understood, the reproducibility of experimental data points was somewhat erratic for this particular sample. It should be pointed out, however, that there is considerable uncertainty in estimating d_{rss} for systems containing short H–H distances, as discussed in Sec. II, so the exact coincidence of experimental and simulated points may be somewhat fortuitous. This is, of course, independent of the question of how successfully ^{1}H linewidths in these intermediate geometry systems can be reproduced using this simple 2-spins-per-cell model.

C. 1D lattice: d_4-urea·decanoic acid inclusion system

As discussed above, a purely one-dimensional geometry is a special case as it behaves inhomogeneously under spinning, giving sharp spinning sidebands. The nonzero linewidths obtained for the urea inclusion system in Fig. 2 are a result of weak couplings between protons in different urea tunnels plus coupling to unsubstituted hydrogens in the nominally 100% d_4-urea. Since the observed spin-echo linewidths only reflect small deviations from the ideal geometry, there is little interest in trying to model this system.

It is interesting, however, to consider the effect of small deviations away from the linear geometry as this will turn an initially inhomogeneous system (with zero linewidth) into a "normal" homogeneous system with finite linewidth. Figure 6 illustrates this transition using a one-dimensional lattice of spin pair unit cells. When the spin pair internuclear vector is aligned along the translation axis, the system behaves inhomogeneously and the sidebands have zero width. But only small deviations from this geometry are required for the linewidth to increase sharply. In this case, the system behaves homogeneously for angles above 15° (similar curves are ob-

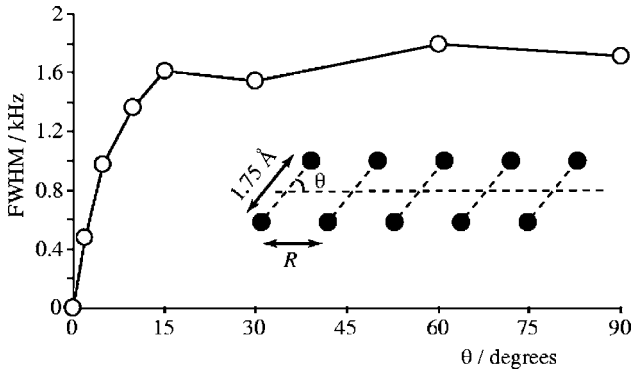

FIG. 6. Investigating the transition between inhomogeneous and homogeneous network geometries using a system of five cells of two spins separated by 1.75 Å. The intercell distance was adjusted to maintain a constant d_{rss} of 25.7 kHz as the angle between the spin pair and the translation axis, θ, was varied. This geometry and d_{rss} is chosen to approximate that of an alkane chain for $\theta=90°$.

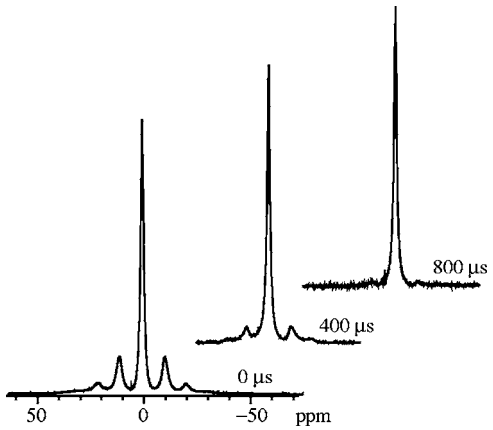

FIG. 7. 500 ^{1}H NMR spectra of adamantane spinning at 5 kHz following a spin echo as a function of spin-echo period. The maximum intensity is normalized, showing clearly that the spinning sidebands decrease in intensity more quickly than the centerband.

tained for different ratios of intracell and intercell distances). Analogous behavior has previously been observed in small (three) spin model systems.[10]

As an aside, the inhomogeneous nature of the Hamiltonian makes these ideal samples for adjusting the magic angle since the linewidth is extremely sensitive to magic angle misset. The high mobility also results in reasonably short relaxation times (typical recycle delays are a few seconds), facilitating direct optimization on the sample. The effects of magic-angle misset on ^{1}H linewidths in more typical systems can be neglected, provided that the magic angle has been verified on sensitive samples such as this one or more classical setup samples, such as KBr.

D. Center band versus sideband linewidths

As seen earlier in Fig. 3, center bands and sidebands have different characteristics for a homogeneous Hamiltonian. This is also clearly visible experimentally in Fig. 7 which shows ^{1}H MAS spectra of adamantane as a function of the spin-echo delay (Fig. 1). The sideband intensity decays significantly more quickly than that of the center band. Curiously, despite adamantane being an extremely well-studied model system and the distinction between center band and sideband characteristics having been made theoretically,[12] this experimental behavior seems not to have been previously discussed in the literature.

Simulations on periodic model systems provide some insight into this behavior. As shown in Fig. 8(b), simple ^{1}H spectra calculated for different crystallite orientations are surprisingly different despite the cubic symmetry of the lattice. In general, the shape and intensity of the center band is distinctly different from those of the sidebands. At certain orientations, the internuclear vectors between otherwise strongly coupled spins lie close to the magic angle with respect to the magnetic field, and so the effective coupling strength is relatively small, resulting in spectra dominated by the center band and with relatively weak, but sharp sidebands (dashed line). At other orientations, the effective coupling strength is larger, and the sidebands are broader and more significant (solid line). The larger effective coupling will also be associated with a more rapid decay in spin-echo experiments. Although the linewidth and decay rate are both determined by the strength (and nature) of the coupling network, the connection between linewidth and spin-echo decay rate is not necessarily direct. This contrasts with linewidth due to T_2 relaxation in solution-state NMR where there is a direct reciprocal relationship between the width of a resonance and the time constant for its decay (FWHM$=1/\pi T_2$).

To consider the effective coupling strength for individual crystallite orientations (as opposed to an average over an isotropic powder), we must include the dependence of the dipolar coupling on the orientation between the internuclear vector and the magnetic field, θ, when calculating the effective coupling strength,

$$d^{\Omega}_{\mathrm{rss},j} = \sqrt{\sum_{k\neq j} d^{\Omega}_{jk}} = \sqrt{\sum_{k\neq j} \frac{3(\cos^2\theta - 1)d^2_{jk}}{2}}, \qquad (8)$$

where $d^{\Omega}_{\mathrm{rss}}$ is used to distinguish the effective coupling

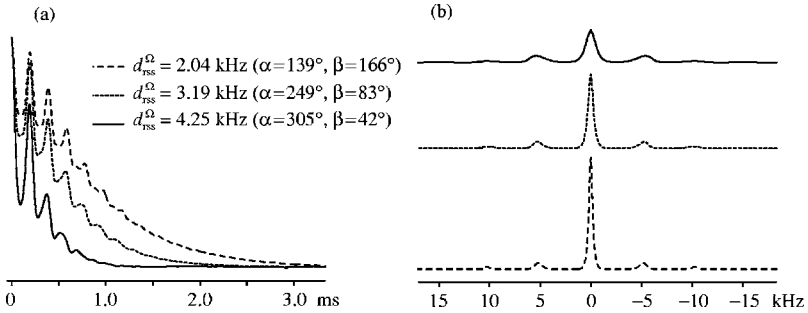

FIG. 8. (a) Simulated ^{1}H free induction decays and (c) spectra for three sample crystallite orientations. The simulations used the same nine spin quasi-3D model of Fig. 3.

strength for an *individual crystallite orientation*, Ω, from the orientation-independent d_{rss} which is appropriate when considering the effective coupling strength for an isotropic powder. d_{rss}^{Ω} averaged over an isotropic distribution of crystallite orientations is simply proportional to d_{rss}.[20] The ratio between the maximum and minimum values of d_{rss}^{Ω} thus quantifies the dependence of the effective coupling strength on crystallite orientation. This ratio is infinite for one-dimensional geometries, since $\min(d_{rss}^{\Omega})=0$, but is still surprisingly large (about 2.5) for spins arranged in a simple cubic lattice.

Hence, although sidebands and center bands have similar widths for a given crystallite orientation, Fig. 8(b), this is not the case in the sum spectrum. The center band contains a higher proportion of intensity from orientations with low d_{rss}^{Ω} values. As a result, it is markedly sharper in the spectrum and also decays at a slower rate compared to the sidebands (i.e., its spin-echo linewidth is also narrow).

Figure 8 also illustrates the limitations of the descriptions of multispin dynamics in terms of stochastic spin diffusion processes. Although such descriptions may be able to *model* signals from orientationally averaged samples, it is clear that the underlying dynamics are significantly more complex. While fitting experimental spin-echo decays from powder samples to simple exponential functions is a useful means of parametrizing the dynamics of a multispin system (and is perhaps surprisingly successful), it is important to remember that the resulting T_2 is a phenomenological quantity with limited physical significance.

IV. INHOMOGENEOUS CONTRIBUTIONS TO ^{1}H LINEWIDTHS

The previous section considered the factors determining the underlying homogeneous linewidth in ^{1}H MAS line shapes (as measured by spin-echo experiments). This was seen to be determined by the strength of the dipolar coupling network relative to the sample spinning rate. This section considers inhomogeneous contributions to the linewidth, i.e., those components that are refocused by a spin echo. As the inhomogeneous contribution cannot be measured directly, we define it here as the difference between the natural FWHM linewidth and the spin-echo linewidth obtained from fitting the spin-echo decay to a phenomenological T_2. As discussed above, this fitting has its limitations and so the absolute values for the resulting inhomogeneous contributions should be interpreted with care, especially when the homogeneous contribution is dominant and/or the decay fits poorly to a simple exponential. This can lead to occasional examples where the spin-echo linewidth appears to be *larger* than the full natural linewidth. The inhomogeneous linewidth can also be estimated by extrapolating plots of natural linewidth versus $1/\nu_r$ to infinite spin rate,[30] but this approach has its own limitations as such plots are not necessary linear [Fig. 9(a)].

Figure 9 shows the effect of magic-angle spinning on the ^{1}H linewidth of HMB. Here, aromatic ring currents and a high degree of π stacking in the crystal structure mean that the magnetic susceptibility of the crystalline solid is strongly anisotropic, i.e., its anisotropy of the bulk magnetic susceptibility (ABMS) ($\Delta\chi$) is particularly large. Although all solid samples experience susceptibility broadening due to variations in the bulk susceptibility from crystallite boundaries, voids, etc., these are averaged away by magic-angle spinning *if* the material itself has an isotropic susceptibility (i.e., $\Delta\chi=0$). Magic-angle spinning is only partially effective, however, for materials with a nonzero ABMS,[31,32] resulting in broadened lines for powder samples even under MAS. The large ABMS in hexamethylbenzene manifests itself as a large difference between the spin-echo and natural width [Fig. 9(a)]. As expected, this inhomogeneous linewidth is independent of the spinning rate [Fig. 9(b)], but scales with the magnetic field, i.e., is constant when expressed in ppm. This contrasts with the spin-echo linewidth [Fig. 9(c)], which is, to a good approximation, independent of magnetic field (when expressed in frequency units) and is strongly dependent on the MAS rate.

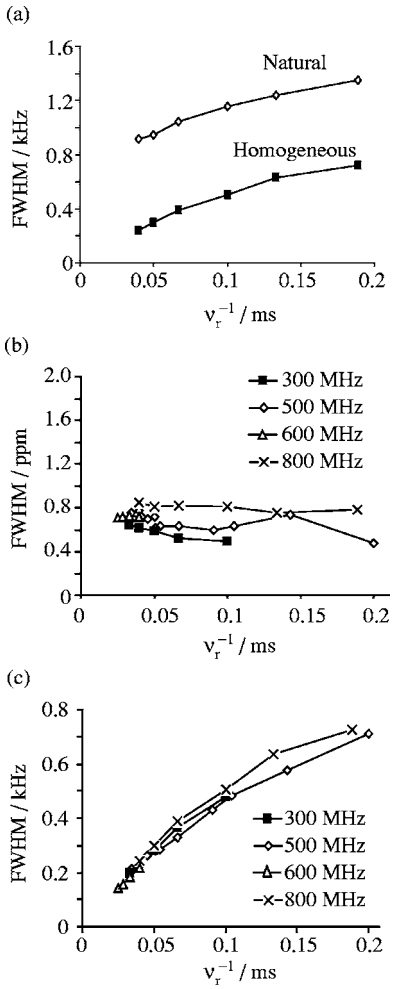

FIG. 9. Linewidth contributions for the ^{1}H MAS spectrum of hexamethylbenzene as a function of spinning rate: (a) natural FWHM and spin-echo linewidths at a proton NMR frequency of 800 MHz; (b) inhomogeneous and (c) spin-echo linewidths measured in different magnetic fields. The inhomogeneous component scales with B_0 (i.e., is constant in ppm), while the homogeneous component is independent of the static field strength.

These magnetic susceptibility broadenings are often the limiting factor in dilute-spin solid-state NMR,[32,33] and previous studies of ^{1}H natural linewidths as a function of spin rate and static magnetic field have suggested that they are also

TABLE III. Inhomogeneous linewidths estimated from the difference between natural and spin-echo linewidths from experiments at 500 MHz ^{1}H Larmor frequency. ^{13}C data were obtained from CP/MAS experiments, while ^{1}H data were acquired from samples spinning at 20 kHz.

Compound	^{13}C (ppm)	^{1}H (ppm)
Naphthalene	1.8	1.9
Hexamethylbenzene	1.2	0.7

limiting for ^{1}H NMR under MAS.[30] Our own measurements tend to support this proposition. Table III shows estimates of the inhomogeneous linewidths for two samples where the difference between the spin-echo and natural linewidth is large enough to enable reasonable estimates of the inhomogeneous linewidth to be made. Even in these cases, the values are estimates due to the systematic errors in modeling the spin-echo decays from both ^{1}H and ^{13}C data as single exponentials; e.g., spin-echo decay rates from decoupled ^{13}C spectra have been shown to vary with the ^{1}H decoupling method.[34] For comparison, an estimated value of about 0.3 ppm was obtained in Ref. 30 for a more typical organic compound, malonic acid, by extrapolating from data points acquired at very high spin rates and static magnetic field.

Most sources of the inhomogeneous contributions, such as susceptibility broadenings, inhomogeneities of the bulk magnetic field, etc., will be identical for all nuclei. Hence the inhomogeneous broadenings for different NMR nuclei in a sample are expected to be approximately constant (when expressed in ppm). Table III shows estimates of the inhomogeneous linewidths for ^{13}C and ^{1}H NMRs of a pair of samples with substantial inhomogeneous broadenings (essentially due to ABMS effects). This confirms that inhomogeneous linewidths are essentially the same in ppm (or, equivalently, scale with the magnetogyric ratio if expressed in frequency units). The agreement is less good for the sample with the smaller inhomogeneous contribution (HMB), which probably reflects the uncertainties in the estimations.

Inhomogeneous contributions to dilute-spin linewidths have been studied in detail for ^{13}C MAS NMR,[32,33] and so it is not necessary to revisit this existing work, given that the inhomogeneous broadenings are seen to be the same on both rare and abundant spins. It should be noted, however, that a broadening of, say, 0.3 ppm due to susceptibility effects or sample disorder has a much smaller impact on ^{13}C NMR, with its large chemical shift range, in comparison to ^{1}H NMR. Hence in many cases the intrinsic inhomogeneous broadenings associated with powdered solids may represent an ultimate limit on the resolution of one-dimensional ^{1}H NMR.[30] Similar figures for inhomogeneous broadenings of $\sim$0.2 ppm or less[24,25] have recently been observed for samples of microcrystalline proteins which have been partially deuterated to reduce the homogeneous linewidth. As inhomogeneous broadening factors are largely insensitive to isotopic substitution, this suggests that the inhomogeneous linewidths are intrinsically low for these samples, which is encouraging for future solid-state NMR studies of this important class of systems.

Although the inhomogeneous linewidth will set the ultimate limit on resolution in simple one-dimensional ^{1}H spectra (including those obtained with homonuclear rf decoupling to suppress the ^{1}H dipolar couplings), it is important to remember that the performance of many important experiments is limited by homogeneous linewidth. For instance, J couplings can be measured,[35,36] and exploited for polarization transfer,[37,39] provided they are of least similar magnitude as the spin-echo linewidth, irrespective of whether they are resolved in the one-dimensional spectrum.

V. THE INFLUENCE OF CHEMICAL SHIFTS ON ABUNDANT-SPIN LINEWIDTHS

The previous sections have considered the proton spin system simply in terms of the dipolar couplings between the spins and ignored any potential influence of chemical shifts. This is a common assumption when dealing with abundant, strongly coupled spins and largely justified by the small ^{1}H chemical shift range in typical organic systems. In particular, the spread within crowded regions of spectrum, e.g., alkyl and aromatic regions, is extremely small in comparison with the dipolar linewidth. A 2 ppm shift difference at a Larmor frequency of 800 MHz, for example, corresponds to a frequency difference of only 1.6 kHz, in comparison to a typical dipolar linewidth of $\sim$100 kHz. The success of models based purely on the dipolar coupling in explaining the linewidths of individual samples and rationalizing the behavior of a wide range of proton-containing compounds, as described in Sec. III, is a strong indicator that chemical shift effects can be neglected as a factor in ^{1}H resolution.

It is interesting to consider, however, the trends that would be observed if the balance between the magnitude of the chemical shift and dipolar coupling Hamiltonians were shifted, e.g., if working at extremely high magnetic field or studying abundant nuclei with a much larger chemical shift range, such as ^{19}F. This section considers, firstly, the influence of large differences in isotropic chemical shift and, secondly, "rotational resonance" effects associated with significant chemical shift anisotropies (CSA) on the ^{1}H linewidth.

As discussed above, it is rare to encounter differences in isotropic chemical shift between coupled protons that are significant in comparison to the local coupling strength. Trial simulations confirm that typical ^{1}H shift differences (of up to 10 ppm at a Larmor frequency of 500 MHz) have no significant effects on linewidth in typical organic solids (using d_{rss} values of about 20 kHz). However, there are a few examples in the literature where partial averaging of the dipolar couplings or unusually large chemical shifts have shifted the balance towards the limit where the shift differences exceed the coupling strength. If we consider, for example, a dipolar coupled spin pair with a difference in NMR frequencies of Δ, the nuclear spin Hamiltonian is

$$H(t) = \frac{\Delta}{2} I_{1z} - \frac{\Delta}{2} I_{2z} + d(t)\left[2I_{1z}I_{2z} + \frac{1}{2}(I_{1+}I_{2-} + I_{1-}I_{2+}) \right]. \tag{9}$$

In the limit that $\Delta \gg d$, the Hamiltonian will be truncated to terms that commute with the chemical shift Hamiltonian; i.e., the "flip-flop" term of Eq. (9) can be neglected to leave an

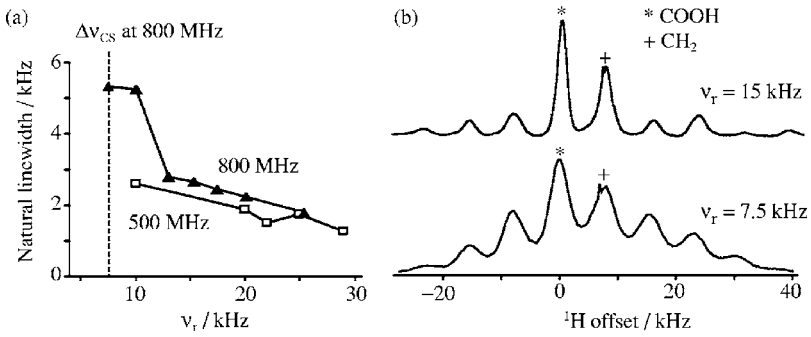

FIG. 10. Example of rotational resonance in ^{1}H NMR using a sample of powdered malonic acid. The chemical shift difference between the methylene and carbonyl resonances is about 9.4 ppm, corresponding to $\Delta\nu = 7.5$ kHz at a ^{1}H Larmor frequency of 800 MHz. (a) ^{1}H FWHM linewidths of the methylene resonance as a function of MAS rate at 800 and 500 MHz; (b) sample spectra at 800 MHz and spinning rate of 7.5 kHz (rotational resonance with $n=1$) and 15 kHz (far from resonance condition).

effective dipolar Hamiltonian identical in form to the heteronuclear dipolar coupling Hamiltonian,

$$H(t) = \frac{\Delta}{2}(I_{1z} - I_{2z}) + 2d(t)I_{1z}I_{2z}. \tag{10}$$

As such a Hamiltonian is always self-commuting, $[H(t),H(t')]=0$, it is inhomogeneous under magic-angle spinning and gives sharp spinning sidebands (Sec. I). In the intermediate case, where the differences in NMR frequencies are comparable to the dipolar linewidth, the ^{1}H linewidth is expected to decrease as the square of the spinning rate,[40] i.e., much faster than observed for systems where chemical shift differences are negligible.

The sample in Ref. 41, for example, contains two H types: H atoms in a mobile hydrogen molecule and relatively immobile hydrogens in the surrounding cage. In the absence of sample spinning, the sites are coupled to form an extended network, as shown by a featureless ^{1}H spectrum and a common T_1 relaxation time. Only modest spinning, however, is sufficient to suppress the weak residual couplings between mobile hydrogen and the cage. As the two spin types have very different chemical shifts (a difference of about 15 ppm), we would expect the two "reservoirs" to be decoupled from each other. The resulting spectrum is the sum of extremely sharp peaks from the H_2 and much broader peaks from the rigid cage, and distinct values of T_1 are observed for the different sites.

Alternatively, the chemical shift range of the ^{1}H sites may be unusually large. Paramagnetic shifts in systems containing unpaired electrons, for example, can result in isotropic and anisotropic ^{1}H shifts that are two to three orders of magnitude larger than in typical diamagnetic compounds. In these cases, ^{1}H linewidths improve very rapidly with increasing spinning rate.[42,43]

Rotational resonance is another mechanism by which chemical shift differences can influence line shapes in magic-angle spinning NMR.[40,44,45] This occurs if the difference in resonance frequencies $\Delta\nu$ between two coupled spins matches to a small multiple n of the MAS rate. While rotational resonances with $n>0$ (typically $n=1$ or $n=2$) are easily achieved in, say, ^{13}C-solid-state NMR, they are not commonly encountered in proton NMR since the small ^{1}H chemical shift differences and the high spin rates required for useful ^{1}H resolution make the matching conditions difficult to achieve. As the static magnetic field increases, however, rotational resonance effects may be observed more readily. Figure 10, for example, shows a marked line broadening of the CH_2 resonance at the $n=1$ resonance at a ^{1}H Larmor frequency of 800 MHz.

The $n=0$ rotational resonance is an interesting case where two coupled spins have the same isotropic shifts, but their CSAs have different parameters, e.g., orientation of principal axes. This creates a Hamiltonian which does not commute with itself at different points in the rotor cycle i.e., is homogeneous. This is expected to occur readily for, say, CH_2 units in solids since the isotropic chemical shift differences between the protons will tend to be small (in the absence of ring current effects),[46] while the CSA orientations will be different. Such a rotational resonance has a dramatic effect on the line shape in simple spin pair systems.[40] Figure 11 explores whether the same behavior is observed for abundant-spin systems. In this case where the Hamiltonian is intrinsically homogeneous, the effect is much less dramatic; the CSA needs to be unrealistically large (in proton terms) before it has a noticeable effect on the spectrum [Figs. 11(c) and 11(d)]. In other words, the $n=0$ rotational resonance has

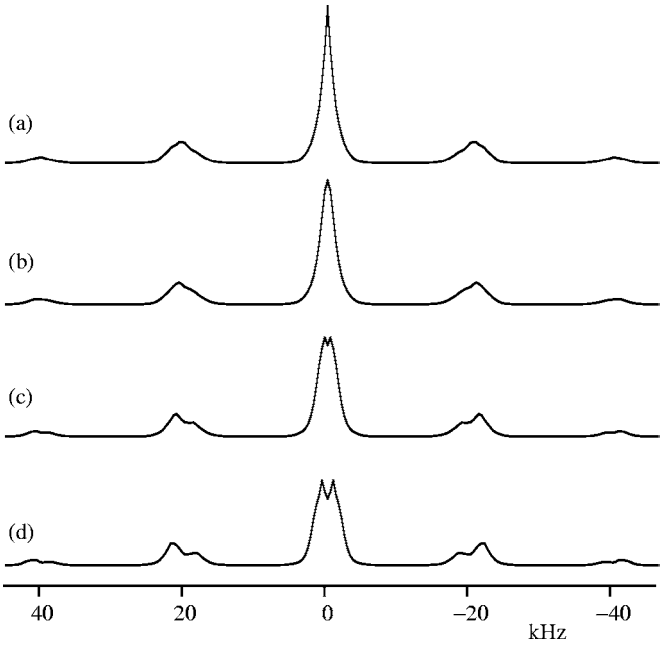

FIG. 11. Effect of the $n=0$ rotational resonance on simulated ^{1}H MAS spectra, using a model system of five cells with two spins per cell and a 20 kHz MAS rate. Distances were set to 1.75 Å within the cell and 2.5 Å between cells. The anisotropies of the chemical shift for both spins were equal to (a) 0 kHz, (b) 3 kHz, (c) 6 kHz, and (d) 10 kHz (asymmetry of zero). The CSA tensors are oriented at 109° between spins and perpendicular to the intercell vector. 144 crystal orientations were simulated in the frequency domain with spectral resolution of 390 Hz.

little impact on a system that is already homogeneous. These effects should be more significant for abundant nuclei with larger CSAs, although in practice it may be difficult to distinguish between a small broadening due to rotational resonance and those due to dipolar couplings since they have essentially the same dependence on the MAS rate (falling as the inverse of spin rate).

In summary, the effects of chemical shift variations do not appear to have a significant impact on ^{1}H resolution in the solid state, confirming the common assumption that only the dipolar coupling network is important. Significant effects can be observed in some atypical systems, or for abundant spins where the ratio of the dipolar linewidth to the size of the shift variations is smaller, such as ^{19}F and ^{31}P.

VI. CONCLUSIONS

Understanding the dynamics of extended networks of dipolar coupled nuclear spins under magic-angle spinning is a difficult problem. The system Hamiltonian is homogeneous in the sense that it does not commute with itself at different times, and so analytical treatments of the dynamics either become intractable in the case of exact treatments (e.g., using the Floquet theory) or invoke empirical factors such as "memory functions." Conventional numerical simulations, on the other hand, are limited in the number of coupled spins they can handle, creating the secondary problem of how to select, say, ten spins from an extended network without the results being distorted by boundary effects.

Numerical simulation with model systems with one-dimensional periodic symmetry has allowed boundary effects to be avoided and greatly increased the efficiency of the calculations. Systematic experiments to measure the ^{1}H linewidths of a variety of model systems as a function of magic-angle spinning rate have provided a comprehensive set of experimental points to compare with simulations. The intrinsic homogeneous linewidth (as measured by spin-echo experiments) was found to follow clear trends, and the experimental values were reproduced in simulations based on structural data from independent diffraction studies. Most notably, the linewidths were found to decrease approximately linearly with increasing spin rate with the gradient depending on overall dipolar coupling strength for a given site, d_{rss}, and geometrical factors which could be rationalized in terms of the dimensionality of network geometry. Bearing in mind that these results are obtained from powder samples and so represent some average over the different crystallite orientations, the calculation of the gradient (G) factors may be amenable to analysis. While the physical significance of the three-dimensional and "one-dimensional" lattices is easy to appreciate, the significance of the intermediate cases may be a fruitful direction for future enquiry—could, for instance, the "G factor" for a stochastic distribution of spins be calculated analytically?

Significantly, it was not possible to measure limits on the spin-echo linewidth due to the relaxation processes that limit linewidths in solution-state NMR, suggesting that there is significant room for developing experiments which are currently limited by decoherence, e.g., by faster magic-angle spinning rates or using deuterium substitution to dilute the proton spin system and so reduce d_{rss} (as well as scaling residual linewidths due to J couplings by $\gamma(^{1}\mathrm{H})/\gamma(^{2}\mathrm{H}) \approx 6.5$).

The resolution limit in simple one-dimensional NMR experiments is set by the inhomogeneous linewidth which varies substantially between samples, from negligibly small for systems such as adamantane to over 1 ppm for samples with a highly anisotropic magnetic susceptibility. This contribution was confirmed to be essentially independent of the nucleus under study, but this limit will have a much larger impact on proton NMR resolution due to the small ^{1}H chemical shift range. The small ^{1}H NMR chemical shift range also meant that chemical shift effects were found to have negligible impact on ^{1}H resolution.

As discussed in Sec. IV, it is important to remember that the performance of many important solid-state NMR experiments is limited by the rate of the underlying homogeneous magnetization decay, rather than the simple one-dimensional resolution. Fast magic-angle spinning, especially in combination with isotopic dilution, will lead to direct improvements in experimental efficiency in these cases. Moreover techniques involving tailored rf pulse sequences, such as FSLG,[47] PMLG,[48] and DUMBO,[49] are, in principle, capable of suppressing the ^{1}H dipolar couplings with much greater efficiency than simple MAS (albeit at the cost of significantly increased experimental complexity). We are currently applying the same principles used in this study to the challenging problem of understanding ^{1}H resolution under both MAS and rf irradiation.

ACKNOWLEDGMENTS

This work was supported under Grant No. GR/S56993/01 from the Engineering and Physical Sciences Research Council. One of the authors (S.P.B.) also thanks the EPSRC for the award of an Advanced Research Fellowship and for Grant No. (GR/S47403/01). The authors thank Ago Samoson (Tallinn, Estonia) for supplying the 1.8 mm probe. The grant holders are thanked for access to the 800 MHz spectrometer.

[1] M. M. Maricq and J. S. Waugh, J. Chem. Phys. **70**, 3300 (1979).
[2] S. P. Brown and H. W. Spiess, Chem. Rev. (Washington, D.C.) **101**, 4125 (2001).
[3] I. Schnell, S. P. Brown, H. Yee-Low, H. Ishida, and H. W. Spiess, J. Am. Chem. Soc. **120**, 11784 (1998).
[4] R. K. Harris, P. Y. Ghi, R. B. Hammond, C.-Y. Ma, and K. J. Roberts, Chem. Commun. (Cambridge) **2003**, 2834.
[5] S. P. Brown, X. X. Zhu, K. Saalwächter, and H. W. Spiess, J. Am. Chem. Soc. **123**, 4275 (2001).
[6] T. M. Alam, M. Nyman, B. R. Cherry, J. M. Segall, and L. E. Lybarger, J. Am. Chem. Soc. **126**, 5610 (2004).
[7] S. P. Brown, I. Schnell, J. D. Brand, K. Müllen, and H. W. Speiss, J. Am. Chem. Soc. **121**, 6712 (1999).
[8] S. P. Brown, I. Schnell, J. D. Brand, K. Müllen, and H. W. Spiess, J. Mol. Struct. **521**, 179 (2000).
[9] S. P. Brown, T. Schaller, U. P. Seelbach, F. Koziol, C. Ochsenfeld, F.-G. Klärner, and H. W. Spiess, Angew. Chem., Int. Ed. **40**, 717 (2001).
[10] E. Brunner, D. Freude, B. C. Gerstein, and H. Pfiefer, J. Magn. Reson. (1969-1992) **90**, 90 (1990).
[11] C. Filip, X. Filip, D. E. Demco, and S. Hafner, Mol. Phys. **92**, 757 (1997).
[12] C. Filip, S. Hafner, I. Schnell, D. E. Demco, and H. W. Spiess, J. Chem.

Phys. **110**, 423 (1999).
[13] S. Ray, E. Vinogradov, G.-J. Boender, and S. Vega, J. Magn. Reson. **135**, 418 (1998).
[14] M. Mehring, *Principles of High Resolution NMR in Solids*, 2nd ed. (Springer, New York, 1983).
[15] T. Charpentier, F. S. Dzheparov, J.-F. Jacquinot, and J. Virlet, Chem. Phys. Lett. **352**, 447 (2002).
[16] M. Ernst, H. Zimmermann, and B. H. Meier, Chem. Phys. Lett. **317**, 581 (2000).
[17] M. Veshtort and R. G. Griffin, J. Magn. Reson. **178**, 248 (2005).
[18] P. Hodgkinson, D. Sakellariou, and L. Emsley, Chem. Phys. Lett. **326**, 515 (2000).
[19] V. E. Zorin, S. P. Brown, and P. Hodgkinson, Mol. Phys. **104**, 293 (2006).
[20] A. Abragam, *Principles of Nuclear Magnetism*, (Oxford University Press, New York, 1961), Chap. IV, pp. 97–132.
[21] Y. Ishii, T. Terao, and S. Hayashi, J. Chem. Phys. **107**, 2760 (1997).
[22] K. D. M. Harris, *Interfacial Science of Solid Host-Guest Systems*, Chemistry for the 21st Century (Blackwell Science, 1997), Chap. 2, pp. 21–55.
[23] B. Reif and R. Griffin, J. Magn. Reson. **160**, 78 (2003).
[24] D. H. Zhou, D. T. Graesser, W. T. Franks, and C. M. Rienstra, J. Magn. Reson. **178**, 297 (2006).
[25] V. Chevelkov, K. Rehbein, A. Diehl, and B. Reif, Angew. Chem., Int. Ed. **45**, 3878 (2006).
[26] P. Reynolds, Acta Crystallogr., Sect. A: Cryst. Phys., Diffr., Theor. Gen. Crystallogr. **34**, 242 (1978).
[27] M. Hohwy, H. Bildsøe, H. J. Jakobsen, and N. C. Nielsen, J. Magn. Reson. **136**, 6 (1999).
[28] C. E. Hughes, Prog. Nucl. Magn. Reson. Spectrosc. **45**, 301 (2004).
[29] R. Delaplane, W. David, R. Ibberson, and C. C. Wilson, Chem. Phys. Lett. **201**, 75 (1993).
[30] A. Samoson, T. Tuherm, and Z. Gan, Solid State Nucl. Magn. Reson. **20**, 130 (2001).
[31] M. Alla and E. Lippmaa, Chem. Phys. Lett. **87**, 30 (1982).
[32] A. N. Garroway, D. L. VanderHart, and W. L. Earl, Philos. Trans. R. Soc. London, Ser. A **299**, 609 (1981).
[33] D. L. VanderHart, W. L. Earl, and A. N. Garroway, J. Magn. Reson. (1969-1992) **44**, 361 (1981).
[34] G. De Paëpe, N. Giraud, A. Lesage, P. Hodgkinson, and L. Emsley, J. Am. Chem. Soc. **125**, 13938 (2003).
[35] L. Duma, W. C. Lai, M. Carravetta, L. Emsley, S. P. Brown, and M. H. Levitt, ChemPhysChem **5**, 815 (2004).
[36] S. P. Brown and L. Emsley, J. Magn. Reson. **171**, 43 (2004).
[37] M. Baldus and B. H. Meier, J. Magn. Reson., Ser. A **121**, 65 (1996).
[38] A. Lesage, C. Auger, S. Caldarelli, and L. Emsley, J. Am. Chem. Soc. **119**, 7867 (1997).
[39] F. Fayon, G. Le Saout, L. Emsley, and D. Massiot, Chem. Commun. (Cambridge) **2002**, 1702.
[40] M. H. Levitt, D. P. Raleigh, F. Creuzet, and R. G. Griffin, J. Chem. Phys. **92**, 6347 (1990).
[41] M. Carravetta, Y. Murata, M. Murata, I. Heinmaa, R. Stern, A. Tontheva, A. Samoson, Y. Rubin, K. Komatsu, and M. H. Levitt, J. Am. Chem. Soc. **126**, 4092 (2004).
[42] K. Liu, D. Ryan, K. Nakanishi, and A. McDermott, J. Am. Chem. Soc. **117**, 6897 (1995).
[43] N. Wickramasinghe, M. Shaibat, and Y. Ishii, J. Am. Chem. Soc. **127**, 5796 (2004).
[44] T. G. Oas, R. G. Griffin, and M. H. Levitt, J. Chem. Phys. **89**, 692 (1988).
[45] D. P. Raleigh, M. H. Levitt, and R. G. Griffin, Chem. Phys. Lett. **146**, 71 (1988).
[46] C. Ochsenfeld, F. Koziol, S. P. Brown, T. Schaller, U. P. Seelbach, and F.-G. Klärner, Solid State Nucl. Magn. Reson. **22**, 128 (2002).
[47] A. Bielecki, A. C. Kolbert, and M. H. Levitt, Chem. Phys. Lett. **155**, 341 (1989).
[48] E. Vinogradov, P. K. Madhu, and S. Vega, Chem. Phys. Lett. **314**, 443 (1999).
[49] D. Sakellariou, A. Lesage, P. Hodgkinson, and L. Emsley, Chem. Phys. Lett. **319**, 253 (2000).
[50] see EPAPS Document No. E-JCPSA6-125-031638 for tables of experimental results for all compounds studied. This document can be reached via a direct link in the online article's HTML reference section or via the EPAPS homepage (http://www.aip.org/pubservs/epaps.html).